ACS ORGANIC & INORGANIC Au
AN OPEN ACCESS JOURNAL OF THE AMERICAN CHEMICAL SOCIETY

pubs.acs.org/orginorgau

Article

# Rapid Access to Ironomycin Derivatives by Click Chemistry

Michał Antoszczak, Sebastian Müller, Ludovic Colombeau, Tatiana Cañeque, and Raphaël Rodriguez*

Cite This: *ACS Org. Inorg. Au* 2022, 2, 222–228

Read Online

ACCESS | Metrics & More | Article Recommendations | Supporting Information

**ABSTRACT:** Salinomycin, a natural carboxylic polyether ionophore, shows a very interesting spectrum of biological activities, including selective toxicity toward cancer stem cells (CSCs). Recently, we have developed a C20-propargylamine derivative of salinomycin (ironomycin) that exhibits more potent activity *in vivo* and greater selectivity against breast CSCs compared to the parent natural product. Since ironomycin contains a terminal alkyne motif, it stands out as being an ideal candidate for further functionalization. Using copper-catalyzed azide−alkyne cycloaddition (CuAAC), we synthesized a series of 1,2,3-triazole analogs of ironomycin in good overall yields. The *in vitro* screening of these derivatives against a well-established model of breast CSCs (HMLER $CD24^{low}$/$CD44^{high}$) and its corresponding epithelial counterpart (HMLER $CD24^{high}$/$CD44^{low}$) revealed four new products characterized by higher potency and improved selectivity toward CSCs compared to the reference compound ironomycin. The present study highlights the therapeutic potential of a new class of semisynthetic salinomycin derivatives for targeting selectively the CSC niche and highlights ironomycin as a promising starting material for the development of new anticancer drug candidates.

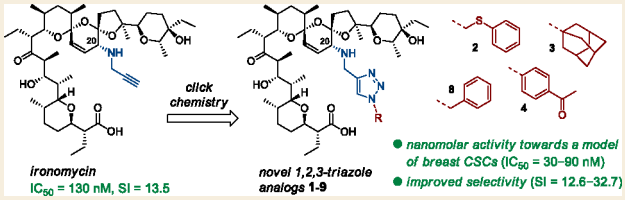


**KEYWORDS:** *polyether ionophores, salinomycin, click reaction, cancer stem cells, anticancer activity*

## 1. INTRODUCTION

Tumors are composed of heterogeneous cell populations that comprise cancer cells and stromal cells, which includes cancer-associated fibroblasts (CAFs), endothelial cells, and immune cells.[1] The paradigm of cancer stem cells (CSCs) defines the existence of rare populations of cancer cells capable of self-renewal, tumor initiation, and maintenance. CSCs are also typically refractory to conventional treatments, are prone to metastatic dissemination, and can cause cancer relapse.[2−8] Thus, the development of new lead structures that can selectively target CSCs is of great interest and represents a potential improvement in the arsenal of modern anticancer treatment strategies.

Salinomycin (**Sal**, Scheme 1), a natural polyether ionophore isolated from *Streptomyces albus*, has been identified in a landmark study by Gupta et al. as a small molecule that preferentially targets breast CSCs.[9] **Sal** reduced the proportion of CSCs by >100-fold relative to that of paclitaxel, a widely used drug in breast cancer therapy.[9] Importantly, **Sal** has also been shown in clinical pilot studies to have therapeutic potential in cancer patients by inducing partial regression of therapy-resistant and heavily pretreated tumors.[10] Mechanistically, many pathways and molecular complexes that confer resistance and survival of CSCs have been identified to be significantly modulated after **Sal** treatment. This includes Wnt/$\beta$-catenin, PI3K/Akt/mTOR, K-Ras, as well as Hedgehog signaling.[11−15] With respect to the very promising biological activity of **Sal**, a number of its semisynthetic analog structures have been developed,[16−30] some of which exhibit relevant activity against cancer cells with stemlike characteristics.[25,30−34]

Recently, we have demonstrated that the introduction of the propargylamine moiety to the C20 position of **Sal** (ironomycin, Scheme 1) improves significantly the ability of the parent structure to selectively target breast CSCs, both *in vitro* and *in vivo*.[33] Compared to chemically unmodified ionophore, ironomycin showed ∼10-times higher potency against mesenchymal HMLER $CD24^{low}$/$CD44^{high}$ cells over those deprived of CSC properties, with an $IC_{50}$ value of about 100 nM.[33] The mechanism of action (MoA) of ironomycin and **Sal** underlying their selectivity toward CSCs involves accumulation of these compounds in lysosomes and iron retention in this organelle, which eventually leads to the production of reactive oxygen species (ROS) and cell death consistent with ferroptosis.[33] Since cells in the mesenchymal state are addicted to iron,[35−37] this cell state exhibits a heightened vulnerability to ironomycin and **Sal**.

As ironomycin contains a terminal alkyne moiety, it is an ideal substrate for further chemical transformations to generate products with enhanced anti-CSC activity, which could be of great value for the development of new anticancer lead drugs. In the present work, we describe the rapid access to potent

Received: November 3, 2021
Revised: December 18, 2021
Accepted: December 21, 2021
Published: January 21, 2022

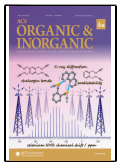

**Scheme 1. Synthetic Access to the 1,2,3-Triazole Analogs of Ironomycin**[a]

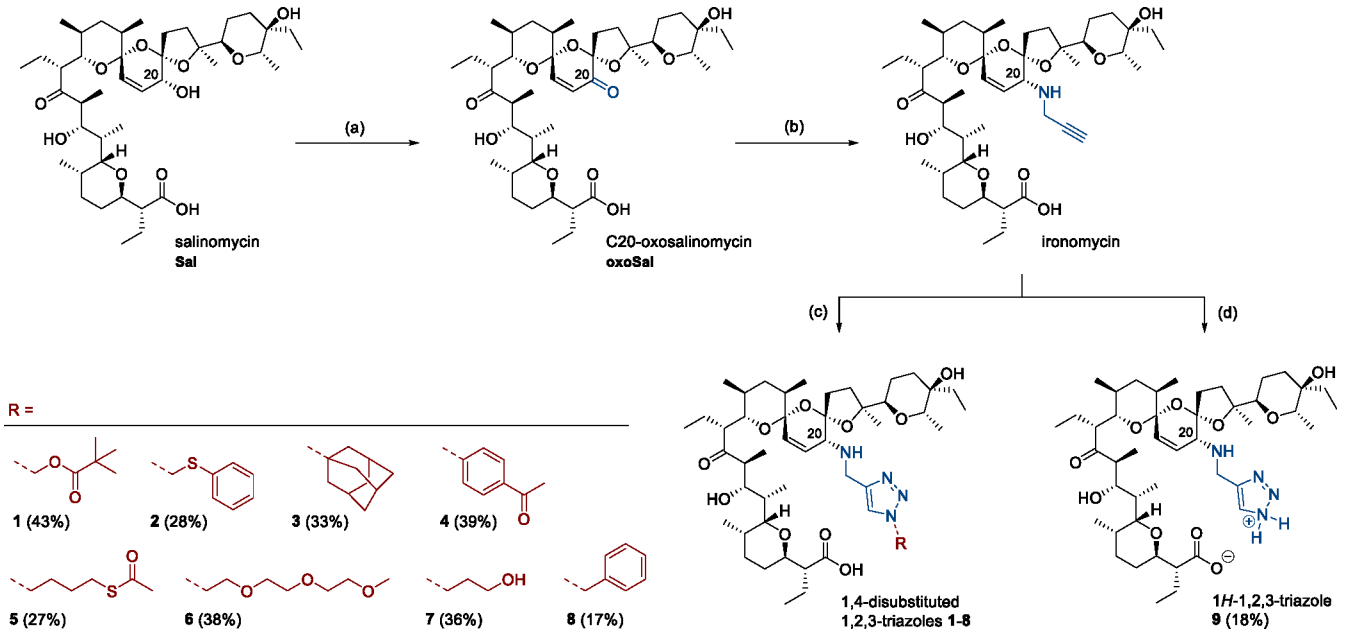


[a]Reagents and conditions: (a) activated $MnO_2$, $CH_2Cl_2$, RT; (b) propargylamine, AcOH, MeOH, RT, then $CeCl_3 \cdot 7H_2O$, $NaBH_3CN$, MeOH, RT; (c) $RN_3$, CuI, DIPEA, ACN, RT; (d) $TMSN_3$, CuI, MeOH/DMF, RT.

**Table 1. Antiproliferative Activity ($IC_{50}$ in $\mu$M) with Standard Deviation and Values of the Selectivity Index (SI) of 1,2,3-Triazole Derivatives of Ironomycin, Measured at 72 h in HMLER $CD24^{low}/CD44^{high}$, HMLER $CD24^{high}/CD44^{low}$, MCF7, and MCF10A Cells**[a]

| | HMLER $CD24^{low}/CD44^{high}$ | HMLER $CD24^{high}/CD44^{low}$ | SI (HMLER) | MCF7 | MCF10A |
|---|---|---|---|---|---|
| ironomycin | 0.13 ± 0.01 | 1.75 ± 0.06 | 13.5 | 0.41 ± 0.07 | 0.12 ± 0.02 |
| **1** | 3.34 ± 0.08 | 10.31 ± 1.00 | 3.1 | 2.91 ± 0.54 | 6.06 ± 0.40 |
| **2** | 0.03 ± 0.004 | 0.98 ± 0.30 | 32.7 | 0.10 ± 0.05 | 2.51 ± 0.71 |
| **3** | 0.03 ± 0.002 | 0.45 ± 0.05 | 15.0 | 0.10 ± 0.05 | 1.26 ± 0.67 |
| **4** | 0.04 ± 0.01 | 0.74 ± 0.17 | 18.5 | 0.43 ± 0.02 | 2.35 ± 1.16 |
| **5** | 0.46 ± 0.03 | 2.42 ± 0.20 | 5.3 | 3.02 ± 0.52 | 12.09 ± 2.00 |
| **6** | 10.85 ± 0.90 | 25.26 ± 2.80 | 2.3 | >12.5 | >12.5 |
| **7** | 8.83 ± 1.10 | 23.71 ± 0.90 | 2.7 | 2.48 ± 0.41 | >12.5 |
| **8** | 0.09 ± 0.02 | 1.13 ± 0.30 | 12.6 | 0.49 ± 0.10 | 0.53 ± 0.23 |
| **9** | 9.29 ± 1.40 | 27.95 ± 2.90 | 3.0 | 12.67 ± 0.18 | 11.98 ± 1.08 |

[a]Selectivity index (SI) was defined as $IC_{50}$(HMLER $CD24^{high}/CD44^{low}$)/$IC_{50}$(HMLER $CD24^{low}/CD44^{high}$). Each $IC_{50}$ value was determined in biological triplicate (three independent biological experiments), and each triplicate was determined in at least technical duplicate.

1,2,3-triazole derivatives of ironomycin obtained by means of click chemistry (Scheme 1). Next, we evaluated the products against a well-established model of breast CSCs, together with the corresponding cancer cells deprived of stemlike characteristics (Table 1). Based on the results, we identified four analogs (**2**−**4** and **8**) that have the ability to preferentially kill CSCs with remarkably low $IC_{50}$ values that compete favorably with ironomycin. All products were also less toxic against normal breast cell line MCF10A compared to ironomycin (Table 1).

## 2. RESULTS AND DISCUSSION

### 2.1. Analog Design and Synthesis

Our key starting material, ironomycin, was synthesized according to a two-step protocol we previously published,[33] with slight modifications. Very briefly, in the first step, the allylic C20-hydroxyl was chemoselectively and quantitatively oxidized to the corresponding C20-ketone (**oxoSal**, Scheme 1), using activated $MnO_2$. Next, **oxoSal** was transformed to obtain the desired product ironomycin via chemoselective and diastereoselective reductive amination, using Luche reaction conditions (Scheme 1). The NMR data of both products **oxoSal** and ironomycin were in agreement with the literature.[33]

To improve the potency and selectivity of **Sal**, Liu and co-workers recently synthesized a series of 1,2,3-triazole analogs at the C1/C20 positions by means of click chemistry.[20] They found that the introduction of the triazole motif at the C20 position can improve the inhibition of breast cancer cell proliferation.[20] On the other hand, Jiang and co-workers generated a library of **Sal** 1,2,3-triazoles with the opposite stereochemistry at the C20 position and further identified a $^{19}F$ MRI sensitive product as a promising agent against cancer cells.[23]

Thus, having access to ironomycin, we synthesized a series of novel 1,2,3-triazole derivatives **1**−**9** (Scheme 1). Regiospecific copper-catalyzed azide−alkyne cycloaddition (CuAAC) of ironomycin with selected commercially available organic azides


https://doi.org/10.1021/acsorginorgau.1c00045
ACS Org. Inorg. Au 2022, 2, 222−228

was successfully completed using the Meldal−Sharpless protocol,[38,39] which led to the diversely 1,4-disubstituted 1,2,3-triazoles **1**−**8** (Scheme 1). To establish a structure−activity relationship (SAR), various organic azides were chosen that give rise to products with various types of substituents, such as shorter or longer aliphatic chains containing heteroatoms (oxygen, sulfur), more sterically hindered *tert*-butyl and adamantane motifs, or aromatic rings. Furthermore, to expand the structural diversity at the C20 position, we also obtained the 1*H*-1,2,3-triazole analog **9** (Scheme 1), following the Cu(I)-catalyzed reaction of ironomycin with $TMSN_3$ in MeOH/DMF.[40] Despite the reactivity of polyfunctionalized molecules, we found that the reactions proceeded cleanly and resulted in the production of nine derivatives with satisfactory yields and in good quantities for further biological evaluation.

The spectral data of compounds **1**−**9** are described in the Supporting Information. In the $^1$H NMR spectra of the target derivatives recorded in $CD_2Cl_2$, the acetylene proton peak observed for ironomycin as a narrow triplet at $\delta$ 2.30 ppm (t, $J$ = 2.0 Hz, 1H) was no longer observed, while a singlet characteristic of a triazole proton was found in the $\delta$ 7.79−8.93 ppm range. With respect to product **9**, the NMR data suggested the zwitterionic nature of the molecule. In particular, in the $^{13}$C NMR spectrum, the signal of the C1 carboxyl group was shifted downfield (184.0 ppm) which is characteristic of a zwitterionic structure, while the singlet observed in the $^1$H NMR spectrum at 4.99 ppm (s, 2H) corresponds to the ammonium group. Finally, HRMS analysis also supported the formation of the expected products, with $[M + H]^+$ as the main peaks.

To study the ionic binding properties of the synthesized derivatives, we investigated whether **2** has the ability to directly interact with iron(II). $^1$H NMR experiments showed that addition of 0.5 equiv of iron(II) chloride to a $CD_3OD$ solution of **2** resulted in line broadening and shifting of specific proton signals, including triazole, thiomethylene, and the C18−C19 olefinic protons (Supporting Information, Figure S28), indicating interactions between **2** and iron(II) in solution. A similar trend was observed for ironomycin previously.[33] Importantly, while **2** was stable under these conditions, chemically unmodified **Sal** has been found to degrade in the presence of iron(III) chloride over time.[33]

### 2.2. Anti-CSC Activity Studies

Next, we screened ironomycin together with the library of 1,2,3-triazole derivatives against mesenchymal HMLER $CD24^{low}/CD44^{high}$ cells, a well-established model of human breast CSCs,[41,42] and compared it with their epithelial counterparts HMLER $CD24^{high}/CD44^{low}$ (Table 1).

Interestingly, we found that the antiproliferative activity of the evaluated products strongly depends on the nature (type) of the substituent attached to the triazole ring. Those containing polar motifs (**1** and **5**−**7**, Scheme 1), including a labile thioester, were essentially less active and less selective than the reference ironomycin; a similar observation was made for the *N*-unsubstituted 1,2,3-triazole analog **9** (Table 1). In this group, compound **6** with ethyl ether units and the hydroxyl-containing product **7** exhibited low cytotoxicity, suggesting that the metal chelation ability is perturbed by these chemical modifications. Conversely, derivatives containing sterically hindered apolar moieties, such as adamantane or aromatic rings (**2**−**4** and **8**, Scheme 1), exhibited up to a 4-fold increase in potency, with an improved selectivity for the mesenchymal state of cells comparable to ironomycin (Table 1). The analogs with adamantane or phenyl substituents showed consistently lower active concentrations in cell viability assays than those with *tert*-butyl or aliphatic motifs. Remarkably, analog **2** was characterized by an $IC_{50}$ value of 30 nM toward HMLER $CD24^{low}/CD44^{high}$ cells and was the most potent of the series. This compound also showed higher selectivity than ironomycin (SI = 32.7 versus 13.5). Compared to the structurally similar analog **8**, compound **2** exhibited improved biological activity; this suggests that the sulfur atom of the thioether group may contribute to iron coordination and/or bring flexibility. It is worth noting that the activity of products **3** and **4** was also improved with lower $IC_{50}$ values compared to ironomycin, yet with comparable SI.

Interestingly, our new family of compounds also showed toxicity against MCF7 breast cancer cells, generally with low $IC_{50}$ values, with **2** and **3** showing $IC_{50}$ values of 100 nM, a 4-fold improvement over reference ironomycin (Table 1). Moreover, we generally observed lower toxicity of these analogs against MCF10A normal breast cells (Table 1), showing a potential therapeutic window to selectively target cancer cells.

## 3. CONCLUSIONS

In summary, the marked antiproliferative effect of ironomycin on the mesenchymal state of cancer cells prompted us to synthesize a series of its 1,2,3-triazole derivatives to further explore potential improvements. The versatile and practical approach described in this study provides a convenient and rapid access to potent semisynthetic small molecules that represent valuable tools for cancer cell biology studies.

All derivatives were assessed for their antiproliferative activity and selectivity for the mesenchymal state of cancer cells using a well-established model of CSCs. Notably, four products (**2**−**4** and **8**) showed more potent activity against HMLER $CD24^{low}/CD44^{high}$ cells compared to the landmark compound ironomycin. Specifically, derivative **2** exhibits one of the highest potencies described thus far against this model cell line, laying down the foundation for the development of new anticancer drugs.

## 4. EXPERIMENTAL SECTION

### 4.1. General Information

Detailed descriptions of the general procedures, equipment, and measurement parameters can be found in the Supporting Information. While C20-oxosalinomycin (**oxoSal**) was synthesized following exclusively the protocol published by us previously,[33] the procedure for the preparation of ironomycin was slightly modified compared to the original one.[33]

Briefly, under argon atmosphere, C20-oxosalinomycin (**oxoSal**; 1.0 g, 1.3 mmol, 1.0 equiv) was dissolved in anhydrous MeOH (50 mL), followed by the addition of activated MS 4 Å, propargylamine (830 $\mu$L, 13.0 mmol, 10.0 equiv), and glacial acetic acid (500 $\mu$L). The yellow solution was stirred for 3 h at RT, prior to the addition of $CeCl_3{\cdot}7H_2O$ (500 mg, 1.3 mmol, 1.0 equiv) and the dropwise addition of a solution of $NaBH_3CN$ (117 mg, 1.8 mmol, 1.4 equiv) in anhydrous MeOH (20 mL) over 20 h at RT, using a syringe pump. After addition of all of the reducing agent, the reaction mixture was stirred for an additional 3 h. Then, the yellow cloudy reaction mixture was filtered to remove the insoluble components. The filtrate was evaporated to dryness, and $CH_2Cl_2$ (40 mL) was added to the yellow oily residue. After mixing, the organic solvent containing ironomycin was filtered off. The filtrate was then extracted twice with an aqueous solution of $H_2SO_4$ (15 mM, 2 × 30 mL) and once with distilled water


https://doi.org/10.1021/acsorginorgau.1c00045
ACS Org. Inorg. Au 2022, 2, 222−228

(30 mL). The organic layer was separated, dried over $MgSO_4$, evaporated under reduced pressure, and purified chromatographically using first the CombiFlash system (cyclohexane/EtOAc 0% → 100%) and then the HPLC equipped with a C18-reverse phase column (gradient: ACN/$H_2O$/FA 1/1/0.1 to ACN/FA 1/0.1) to give the pure product of the reaction, ironomycin as a white amorphous solid (374 mg, 37% yield).

### 4.2. General Procedure for the Preparation of 1,4-Disubstituted 1,2,3-Triazoles of Ironomycin 1−8

The respective organic azide (1.1 equiv) and DIPEA (3.0 equiv) were introduced to a solution of ironomycin (1.0 equiv) in anhydrous ACN under argon atmosphere, followed by the addition of catalytic CuI (0.1 equiv) in one portion. The reaction mixture was stirred at RT, typically for 24 h. After the consumption of the propargyl precursor (TLC control), the organic solvent was evaporated *in vacuo*. The oily residue was then dissolved in a small portion of $CH_2Cl_2$ and extracted a few times with 10% aq EDTA solution. The organic phases were separated and concentrated under reduced pressure. Purification on silica gel using the CombiFlash system followed by HPLC equipped with a C18-reverse phase column (gradient: ACN/$H_2O$/FA 1/1/0.1 to ACN/FA 1/0.1) gave the pure products of the click reaction, **1−8** (17−43% yield) as amorphous solids. The NMR and HRMS spectra of compounds **1−8** are included in the Supporting Information (Figures S1−S24).

**Compound 1.** Yield: 32 mg, 43%. Isolated as a white amorphous solid, > 95% pure by NMR, and a single spot by TLC. $R_f$: 0.68 in $CH_2Cl_2$/acetone 33%. Strain green with PMA; $^1$H NMR (400 MHz, $CD_2Cl_2$) $\delta$ 8.29 (s, 1H), 6.30 (d, $J$ = 10.3 Hz, 1H), 6.17 (s, 2H), 6.14 (dd, $J$ = 10.2, 4.9 Hz, 1H), 4.64−4.54 (m, 2H), 4.04 (dd, $J$ = 10.1, 1.6 Hz, 1H), 3.96 (dd, $J$ = 10.9, 5.4 Hz, 1H), 3.80−3.71 (m, 2H), 3.65 (dd, $J$ = 10.0, 1.8 Hz, 1H), 3.62 (d, $J$ = 10.2 Hz, 1H), 3.52 (d, $J$ = 5.0 Hz, 1H), 2.86 (dt, $J$ = 10.8, 3.8 Hz, 1H), 2.62−2.50 (m, 2H), 2.14 (ddd, $J$ = 11.6, 8.4, 2.9 Hz, 1H), 2.04−0.62 (m, 65H) ppm; $^{13}$C NMR (101 MHz, $CD_2Cl_2$) $\delta$ 214.7, 179.6, 177.5, 143.6, 129.3, 128.2, 126.8, 106.5, 98.8, 89.0, 77.5, 76.1, 75.7, 73.6, 71.6, 71.2, 70.3, 68.4, 55.7, 54.7, 50.4, 48.7, 42.8, 40.3, 39.8, 39.0, 38.3, 36.3, 32.7, 31.4, 31.0, 29.4, 28.4, 27.0 (3C), 25.2, 23.3, 22.3, 20.4, 17.6, 16.8, 15.7, 14.5, 13.2, 12.8, 12.5, 11.3, 7.2, 6.5 ppm, one signal overlapped; HRMS (ESI$^+$) $m/z$ [M + H]$^+$ Calcd for $C_{51}H_{85}N_4O_{12}$ 945.6159, Found 945.6147.

**Compound 2.** Yield: 26 mg, 28%. Isolated as a white amorphous solid, >95% pure by NMR, and a single spot by TLC. $R_f$: 0.67 in $CH_2Cl_2$/acetone 33%. UV-active and strain green with PMA; $^1$H NMR (500 MHz, $CD_2Cl_2$) $\delta$ 8.23 (s, 1H), 7.41−7.34 (m, 2H), 7.34−7.27 (m, 3H), 6.34 (d, $J$ = 10.2 Hz, 1H), 6.15 (dd, $J$ = 10.1, 5.1 Hz, 1H), 5.62−5.55 (m, 2H), 4.66 (d, $J$ = 13.4 Hz, 1H), 4.58 (d, $J$ = 13.4 Hz, 1H), 4.03 (d, $J$ = 10.0 Hz, 1H), 3.92 (dd, $J$ = 10.5, 5.6 Hz, 1H), 3.79−3.70 (m, 2H), 3.66 (d, $J$ = 9.7 Hz, 1H), 3.59 (d, $J$ = 10.1 Hz, 1H), 3.54 (d, $J$ = 5.0 Hz, 1H), 2.84 (dt, $J$ = 10.8, 3.3 Hz, 1H), 2.62−2.51 (m, 2H), 2.15 (ddd, $J$ = 11.5, 7.3, 4.0 Hz, 1H), 1.99−0.64 (m, 56H) ppm; $^{13}$C NMR (126 MHz, $CD_2Cl_2$) $\delta$ 215.3, 180.0, 143.2, 132.8, 132.6 (2C), 130.2, 129.7 (2C), 128.8, 128.0, 125.6, 106.3, 98.7, 88.9, 77.5, 76.2, 75.7, 73.4, 71.7, 71.2, 68.4, 55.7, 54.6, 50.5, 48.9, 43.1, 40.5, 39.6, 38.2, 36.3, 32.7, 31.6, 31.0, 29.4, 28.5, 27.0, 25.0, 23.3, 22.3, 20.5, 17.6, 16.9, 15.7, 14.5, 13.2, 12.63, 12.61, 11.3, 7.2, 6.6 ppm, one signal overlapped; HRMS (ESI$^+$) $m/z$ [M + H]$^+$ Calcd for $C_{52}H_{81}N_4O_{10}S$ 953.5668, Found 953.5655.

**Compound 3.** Yield: 17 mg, 33%. Isolated as a white amorphous solid, >95% pure by NMR, and a single spot by TLC. $R_f$: 0.49 in $CH_2Cl_2$/acetone 33%. Strain green with PMA; $^1$H NMR (500 MHz, $CD_2Cl_2$) $\delta$ 8.27 (s, 1H), 6.38 (d, $J$ = 10.0 Hz, 1H), 6.25 (dd, $J$ = 9.5, 5.5 Hz, 1H), 4.81 (d, $J$ = 13.1 Hz, 1H), 4.61 (d, $J$ = 13.1 Hz, 1H), 4.07 (d, $J$ = 10.0 Hz, 1H), 3.97 (dd, $J$ = 10.0, 4.9 Hz, 1H), 3.79−3.65 (m, 4H), 3.55 (d, $J$ = 10.0 Hz, 1H), 2.90−2.81 (m, 1H), 2.58−2.48 (m, 2H), 2.28−2.11 (m, 11H), 2.01 (dd, $J$ = 7.9, 5.9 Hz, 2H), 1.91−0.63 (m, 59H) ppm; $^{13}$C NMR (126 MHz, $CD_2Cl_2$) $\delta$ 214.8, 180.3, 140.6, 131.0, 127.9, 122.7, 106.3, 98.7, 88.9, 77.5, 76.5, 75.7, 73.4, 71.6, 71.2, 68.0, 59.6, 55.5, 55.0, 50.6, 49.0, 43.8, 43.2 (3C), 40.8, 39.5, 38.1, 36.3 (3C), 36.2, 32.7, 31.7, 31.0, 30.0 (3C), 29.5, 28.4, 27.0, 24.8, 23.1, 22.2, 20.6, 17.5, 16.8, 15.7, 14.5, 13.2, 12.8, 12.5, 11.3, 7.3, 6.6 ppm; HRMS (ESI$^+$) $m/z$ [M + H]$^+$ Calcd for $C_{55}H_{89}N_4O_{10}$ 965.6573, Found 965.6563.

**Compound 4.** Yield: 27 mg, 39%. Isolated as a white amorphous solid, >95% pure by NMR, and a single spot by TLC. $R_f$: 0.49 in 100% EtOAc. UV-active and strain green with PMA; $^1$H NMR (500 MHz, $CD_2Cl_2$) $\delta$ 8.93 (s, 1H), 8.07 (s, 4H), 6.40 (dd, $J$ = 19.5, 8.8 Hz, 2H), 5.07 (d, $J$ = 12.9 Hz, 1H), 4.86 (d, $J$ = 12.9 Hz, 1H), 4.06 (dd, $J$ = 10.4, 5.8 Hz, 1H), 3.96 (d, $J$ = 9.9 Hz, 1H), 3.81−3.70 (m, 4H), 3.55 (d, $J$ = 10.1 Hz, 1H), 2.96−2.85 (m, 1H), 2.61 (s, 3H), 2.46 (dd, $J$ = 21.1, 8.7 Hz, 2H), 2.20 (ddd, $J$ = 10.8, 8.3, 2.1 Hz, 1H), 2.05−0.60 (m, 53H), 0.38 (d, $J$ = 5.7 Hz, 3H) ppm; $^{13}$C NMR (126 MHz, $CD_2Cl_2$) $\delta$ 216.0, 196.9, 180.5, 143.1, 140.8, 136.8, 131.9, 130.1 (2C), 128.3, 124.9, 120.2 (2C), 106.9, 99.1, 89.2, 77.5, 76.9, 75.9, 73.4, 71.8, 71.1, 68.5, 55.5, 55.4, 50.6, 49.0, 43.9, 41.0, 39.3, 37.9, 36.1, 32.6, 31.5, 31.0, 29.4, 28.5, 27.0, 26.8, 25.0, 23.1, 22.3, 20.6, 17.5, 17.1, 15.6, 14.5, 13.1, 12.6, 12.2, 11.3, 7.2, 6.5 ppm; HRMS (ESI$^+$) $m/z$ [M + H]$^+$ Calcd for $C_{53}H_{81}N_4O_{11}$ 949.5896, Found 949.5883.

**Compound 5.** Yield: 16 mg, 27%. Isolated as a white amorphous solid, >95% pure by NMR, and a single spot by TLC. $R_f$: 0.37 in $CH_2Cl_2$/acetone 33%. Strain green with PMA; $^1$H NMR (400 MHz, $CD_2Cl_2$) $\delta$ 8.22 (s, 1H), 6.36 (d, $J$ = 10.2 Hz, 1H), 6.18 (dd, $J$ = 10.1, 5.5 Hz, 1H), 4.76 (d, $J$ = 13.2 Hz, 1H), 4.65 (d, $J$ = 13.2 Hz, 1H), 4.30 (dt, $J$ = 7.2, 2.2 Hz, 2H), 4.04 (dd, $J$ = 10.2, 1.6 Hz, 1H), 3.95 (dd, $J$ = 10.8, 5.4 Hz, 1H), 3.80−3.71 (m, 2H), 3.67 (dd, $J$ = 10.0, 1.6 Hz, 1H), 3.64 (d, $J$ = 5.5 Hz, 1H), 3.57 (d, $J$ = 10.1 Hz, 1H), 2.86 (ddd, $J$ = 14.6, 11.4, 5.4 Hz, 3H), 2.59−2.50 (m, 2H), 2.30 (s, 3H), 2.17 (ddd, $J$ = 11.7, 8.4, 3.0 Hz, 1H), 2.07−1.15 (m, 34H), 0.96−0.81 (m, 13H), 0.81−0.62 (m, 13H) ppm; $^{13}$C NMR (101 MHz, $CD_2Cl_2$) $\delta$ 215.0, 195.7, 180.1, 141.9, 130.9, 127.9, 126.0, 106.3, 98.7, 88.9, 77.5, 76.4, 75.7, 73.4, 71.6, 71.2, 68.3, 55.6, 54.4, 50.5, 49.9, 49.0, 43.1, 40.7, 39.5, 38.1, 36.2, 32.7, 31.7, 31.0, 30.8, 29.49, 29.46, 28.6, 28.5, 27.0 (2C), 24.9, 23.3, 22.3, 20.5, 17.6, 16.9, 15.7, 14.5, 13.2, 12.6 (2C), 11.3, 7.2, 6.6 ppm; HRMS (ESI$^+$) $m/z$ [M + H]$^+$ Calcd for $C_{51}H_{85}N_4O_{11}S$ 961.5930, Found 961.5920.

**Compound 6.** Yield: 29 mg, 38%. Isolated as a cream amorphous solid, >95% pure by NMR, and a single spot by TLC. $R_f$: 0.20 in $CH_2Cl_2$/acetone 33%. Strain green with PMA; $^1$H NMR (500 MHz, $CD_2Cl_2$) $\delta$ 8.17 (s, 1H), 6.31 (d, $J$ = 10.2 Hz, 1H), 6.12 (dd, $J$ = 10.1, 4.7 Hz, 1H), 4.59 (q, $J$ = 13.4 Hz, 2H), 4.52−4.43 (m, 2H), 4.07 (d, $J$ = 9.9 Hz, 1H), 3.95 (dd, $J$ = 10.6, 5.5 Hz, 1H), 3.86 (t, $J$ = 5.5 Hz, 2H), 3.76 (dt, $J$ = 13.3, 4.8 Hz, 2H), 3.66 (d, $J$ = 9.6 Hz, 1H), 3.64−3.51 (m, 9H), 3.48 (dd, $J$ = 5.6, 3.5 Hz, 2H), 3.32 (s, 3H), 2.85 (dt, $J$ = 10.9, 3.3 Hz, 1H), 2.62−2.50 (m, 2H), 2.20−2.11 (m, 1H), 2.04 (dd, $J$ = 21.3, 10.3 Hz, 1H), 1.99−1.13 (m, 28H), 0.98−0.81 (m, 13H), 0.81−0.62 (m, 13H) ppm; $^{13}$C NMR (126 MHz, $CD_2Cl_2$) $\delta$ 214.7, 179.8, 142.4, 129.5, 127.9, 126.3, 106.2, 98.6, 88.9, 77.5, 76.1, 75.7, 73.5, 72.3, 71.6, 71.2, 71.0, 70.79, 70.76, 69.8, 68.3, 59.0, 55.7, 54.3, 50.40, 50.36, 48.9, 42.8, 40.4, 39.8, 38.3, 36.3, 32.7, 31.5, 31.0, 29.4, 28.5, 27.0, 25.2, 23.4, 22.3, 20.4, 17.6, 16.7, 15.8, 14.4, 13.2, 12.7, 12.5, 11.3, 7.2, 6.6 ppm; HRMS (ESI$^+$) $m/z$ [M + H]$^+$ Calcd for $C_{52}H_{89}N_4O_{13}$ 977.6421, Found 977.6407.

**Compound 7.** Yield: 27 mg, 36%. Isolated as a white amorphous solid, >95% pure by NMR, and a single spot by TLC. $R_f$: 0.16 in $CH_2Cl_2$/acetone 33%. Strain green with PMA; $^1$H NMR (400 MHz, $CD_2Cl_2$) $\delta$ 8.58 (s, 1H), 6.44 (d, $J$ = 10.0 Hz, 1H), 6.31 (dd, $J$ = 10.0, 6.2 Hz, 1H), 4.95 (d, $J$ = 13.2 Hz, 1H), 4.61 (d, $J$ = 13.2 Hz, 1H), 4.55−4.37 (m, 2H), 4.07−3.94 (m, 2H), 3.83−3.62 (m, 4H), 3.54 (d, $J$ = 10.1 Hz, 1H), 3.48 (t, $J$ = 6.1 Hz, 2H), 2.81 (dt, $J$ = 11.0, 3.8 Hz, 1H), 2.60−2.45 (m, 2H), 2.20−2.10 (m, 1H), 2.09−0.56 (m, 59H) ppm; $^{13}$C NMR (101 MHz, $CD_2Cl_2$) $\delta$ 215.0, 180.5, 140.5, 132.2, 128.0, 127.7, 107.0, 99.3, 89.3, 77.5, 77.1, 76.0, 73.3, 71.9, 71.1, 67.9, 58.1, 55.3, 55.2, 50.5, 49.6, 46.6, 43.6, 40.9, 39.3, 38.1, 35.9, 32.7, 32.4, 31.4, 31.0, 29.5, 28.5, 27.0, 24.8, 22.9, 22.2, 20.8, 17.5, 16.9, 15.6, 14.5, 13.1, 12.6, 12.2, 11.4, 7.3, 6.5 ppm; HRMS (ESI$^+$) $m/z$ [M + H]$^+$ Calcd for $C_{48}H_{81}N_4O_{11}$ 889.5896, Found 889.5885.

**Compound 8.** Yield: 8.0 mg, 17%. Isolated as a white amorphous solid, >95% pure by NMR, and a single spot by TLC. $R_f$: 0.47 in $CH_2Cl_2$/acetone 33%. Strain green with PMA; $^1$H NMR (500 MHz, $CD_2Cl_2$) $\delta$ 8.18 (s, 1H), 7.38−7.30 (m, 5H), 6.36 (d, $J$ = 10.2 Hz,


https://doi.org/10.1021/acsorginorgau.1c00045
ACS Org. Inorg. Au 2022, 2, 222−228

1H), 6.20 (dd, $J$ = 10.1, 5.3 Hz, 1H), 5.47 (s, 2H), 4.70 (d, $J$ = 13.4 Hz, 1H), 4.61 (d, $J$ = 13.4 Hz, 1H), 4.02 (dd, $J$ = 10.2, 1.6 Hz, 1H), 3.90 (dd, $J$ = 10.9, 5.6 Hz, 1H), 3.73 (dt, $J$ = 5.7, 5.2 Hz, 2H), 3.68 (dd, $J$ = 10.0, 1.6 Hz, 1H), 3.63 (d, $J$ = 5.4 Hz, 1H), 3.58 (d, $J$ = 10.1 Hz, 1H), 2.85 (dt, $J$ = 10.9, 3.7 Hz, 1H), 2.59−2.52 (m, 2H), 2.14 (ddd, $J$ = 11.9, 7.8, 3.9 Hz, 1H), 1.94−0.64 (m, 56H) ppm; $^{13}$C NMR (126 MHz, $CD_2Cl_2$) $\delta$ 215.3, 180.1, 142.4, 135.7, 130.7, 129.3 (2C), 128.8, 128.5 (2C), 127.7, 126.1, 106.3, 98.8, 88.9, 77.5, 76.3, 75.8, 73.4, 71.6, 71.1, 68.5, 55.6, 54.7, 50.5, 48.9, 43.2, 40.6, 39.6, 38.2, 36.3, 32.7, 31.5, 31.0, 29.4, 28.5, 26.9, 25.0, 23.2, 22.3, 20.5, 17.6, 17.0, 15.7, 14.4, 13.2, 12.6, 12.5, 11.4, 7.2, 6.6 ppm, one signal overlapped; HRMS (ESI$^+$) $m/z$ [M + H]$^+$ Calcd for $C_{52}H_{81}N_4O_{10}$ 921.5947, Found 921.5938.

### 4.3. Synthesis of the 1*H*-1,2,3-Triazole Analog of Ironomycin (9)

Trimethylsilyl azide (28 $\mu$L, 0.21 mmol, 1.5 equiv) was added to an anhydrous DMF/MeOH solution (2.0 mL, 9:1) of catalytic CuI (1.3 mg, 0.007 mmol, 0.05 equiv) and ironomycin (102 mg, 0.14 mmol, 1.0 equiv) under argon in a microwave vial. The reaction mixture was stirred at 100 °C for 6 h. After the consumption of the propargyl precursor (TLC control, mobile phase: cyclohexane/EtOAc 50%), the organic solvents were evaporated *in vacuo*. The oily residue was then dissolved in a small portion of $CH_2Cl_2$ and extracted a few times with 10% aq EDTA solution. The organic phases were separated, dried over $MgSO_4$, and concentrated under reduced pressure. Purification by HPLC equipped with a C18-reverse phase column (gradient: ACN/$H_2O$/FA 1/1/0.1 to ACN/FA 1/0.1) gave the pure product of the click reaction, **9** (18% yield) as a white amorphous solid. The NMR and HRMS spectra of compound **9** are included in the Supporting Information (Figures S25−S27).

**Compound 9.** Yield: 20 mg, 18%. Isolated as a white amorphous solid, >95% pure by NMR, and a single spot by TLC. $R_f$: 0.12 in cyclohexane/EtOAc 50%. Strain green with PMA; $^1$H NMR (400 MHz, $CD_2Cl_2$) $\delta$ 7.79 (s, 1H), 6.55 (d, $J$ = 9.9 Hz, 1H), 6.09 (dd, $J$ = 9.8, 6.5 Hz, 1H), 4.99 (s, 2H), 4.10−4.04 (m, 2H), 3.84 (q, $J$ = 6.9 Hz, 1H), 3.72 (dd, $J$ = 10.6, 3.4 Hz, 1H), 3.67 (dd, $J$ = 10.0, 1.6 Hz, 1H), 3.57 (d, $J$ = 10.3 Hz, 1H), 3.51 (d, $J$ = 6.5 Hz, 1H), 2.80 (dt, $J$ = 11.1, 4.1 Hz, 1H), 2.65−2.55 (m, 2H), 2.34−2.16 (m, 1H), 2.06−0.59 (m, 58H) ppm; $^{13}$C NMR (101 MHz, $CD_2Cl_2$) $\delta$ 217.4, 184.0, 135.2, 134.9, 128.8, 126.8, 106.0, 98.9, 89.6, 77.5, 77.0, 76.1, 73.6, 71.4, 71.1, 68.5, 55.7, 52.5, 50.8, 50.6, 41.7, 39.8, 39.0, 37.7, 35.9, 32.7, 31.2, 30.6, 29.3, 28.7, 27.4, 26.2, 23.1, 22.8, 20.6, 17.6, 17.1, 15.5, 14.4, 13.2, 12.4, 12.0, 11.3, 7.1, 6.5 ppm; HRMS (ESI$^+$) $m/z$ [M + H]$^+$ Calcd for $C_{45}H_{75}N_4O_{10}$ 831.5478, Found 831.5468.

### 4.4. Cell Culture

HMLER cells naturally repressing E-cadherin, obtained from human mammary epithelial cells infected with a retrovirus carrying hTERT, SV40, and the oncogenic allele *H-rasV12*, were cultured in DMEM/F12 (Gibco, 31331-028) supplemented with 10% FBS, 10 $\mu$g mL$^{-1}$ insulin (Sigma-Aldrich, I0516), 0.5 $\mu$g mL$^{-1}$ hydrocortisone (Sigma-Aldrich, H0888), and 0.5 $\mu$g mL$^{-1}$ puromycin (Life Technologies, A11138-02) and were a generous gift from Alain Puisieux (INSERM). All cells were incubated at 37 °C with 5% $CO_2$. HMLER CD44$^{low/high}$ cells stained with CD24-APC and CD44-PE antibodies were sorted by FACS using an Aria IIu (BD Biosciences) to obtain isolated CD24$^{low}$/CD44$^{high}$ and CD24$^{high}$/CD44$^{low}$ cell populations. HMLER CD24$^{low}$/CD44$^{high}$ cells were supplemented with 10 ng mL$^{-1}$ human epidermal growth factor (EGF, Miltenyi Biotec, 130-093-750, 100 ng mL$^{-1}$), while HMLER CD24$^{high}$/CD44$^{low}$ cells were grown without EGF. MCF7 cells (ATCC, HTB-22) were cultured in DMEM GlutaMAX (ThermoFisher Scientific, 61965059) supplemented with 10% FBS (Gibco, 10270-106) and a penicillin−streptomycin mixture (BioWhittaker/Lonza, DE17-602E). MCF10A cells (ATCC, CRL-10317) were cultured in DMEM/F12 supplemented with 10% Horse Serum (Invitrogen, 16050-122), 10 $\mu$g mL$^{-1}$ insulin, 10 ng mL$^{-1}$ EGF, 0.5 $\mu$g mL$^{-1}$ hydrocortisone, 100 ng mL$^{-1}$ cholera toxin (Sigma-Aldrich, C8052), and 1 × PenStrep (Invitrogen, 15070-063).

### 4.5. Cell Viability Assay (IC$_{50}$)

The cell viability assay was carried out by plating 1000 cells per well in 96-well plates. Cells were treated for 72 h in a range between 12 nM and 50 $\mu$M using serial dilutions, following the manufacturer's protocol. Very briefly, CellTiter-Blue reagent (G8081, Promega) was added after 72 h of treatment, and cells were incubated for 3 h before recording fluorescence intensities ($\lambda_{ex}$ 560/20 nm; $\lambda_{em}$ 590/10 nm) using a PerkinElmer Wallac 1420 Victor2Microplate Reader.

The IC$_{50}$ cell viability curves for synthesized compounds against HMLER CD24$^{low}$/CD44$^{high}$, its isogenic cell line HMLER CD24$^{high}$/CD44$^{low}$, MCF7, as well as MCF10A cells are included in the Supporting Information (Figures S29−S31).

## ■ ASSOCIATED CONTENT

### Supporting Information

The Supporting Information is available free of charge at https://pubs.acs.org/doi/10.1021/acsorginorgau.1c00045.

Detailed descriptions of the general procedures, equipment, and measurement parameters. $^1$H NMR, $^{13}$C NMR, and HRMS spectra of the novel 1,2,3-triazole analogs of ironomycin (**1**−**9**), data on the iron(II) binding capacity experiments, and the IC$_{50}$ cell viability curves (PDF)

## ■ AUTHOR INFORMATION


### Corresponding Author

**Raphaël Rodriguez** − *Department of Chemical Biology Institut Curie, CNRS UMR 3666, INSERM U1143, PSL Université 26 rue d'Ulm, 75005 Paris, France;* orcid.org/0000-0001-7668-446X; Phone: +33 648 482 191; Email: raphael.rodriguez@curie.fr

### Authors

**Michał Antoszczak** − *Department of Chemical Biology Institut Curie, CNRS UMR 3666, INSERM U1143, PSL Université 26 rue d'Ulm, 75005 Paris, France; Department of Medical Chemistry Faculty of Chemistry, Adam Mickiewicz University, 61-614 Poznań, Poland;* orcid.org/0000-0003-0877-1726

**Sebastian Müller** − *Department of Chemical Biology Institut Curie, CNRS UMR 3666, INSERM U1143, PSL Université 26 rue d'Ulm, 75005 Paris, France*

**Ludovic Colombeau** − *Department of Chemical Biology Institut Curie, CNRS UMR 3666, INSERM U1143, PSL Université 26 rue d'Ulm, 75005 Paris, France*

**Tatiana Cañeque** − *Department of Chemical Biology Institut Curie, CNRS UMR 3666, INSERM U1143, PSL Université 26 rue d'Ulm, 75005 Paris, France;* orcid.org/0000-0002-1110-0643

Complete contact information is available at: https://pubs.acs.org/10.1021/acsorginorgau.1c00045


### Author Contributions

R.R. directed the research. M.A. designed and synthesized the derivatives. M.A. and S.M. evaluated the compounds *in vitro*. M.A. and. R.R. wrote the article with contributions from S.M., L.C., and T.C.


### Funding

This research was funded by the European Research Council under the European Union's Horizon 2020 research and innovation program grant agreement No 647973 (R.R.), the

Foundation Charles Defforey-Institut de France (R.R.), Ligue Contre le Cancer (R.R. Equipe Labelisée), and Region IdF for NMR infrastructure (R.R.).

### Notes

The authors declare no competing financial interest.

## ■ ACKNOWLEDGMENTS

M.A. thanks the Polish Science Center (NCN) and the Polish National Agency for Academic Exchange (NAWA) for the scholarships under the UWERTURA (2019/32/U/ST4/00092) and the BEKKER program (PPN/BEK/2019/1/00034), respectively, and the Polish Ministry of Science and Higher Education (MNiSW) for the scholarship for outstanding young scientists in the years 2020−2023 (STYP/15/1665/E-336/2020).

## ■ ABBREVIATIONS

ACN, acetonitrile; AcOH, glacial acetic acid; aq, aqueous; CSCs, cancer stem cells; CuAAC, copper-catalyzed azide−alkyne cycloaddition; DMF, *N*,*N*-dimethylformamide; EDTA, ethylenediaminetetraacetic acid; equiv, equivalent(s); EtOAc, ethyl acetate; FA, formic acid; HPLC, high pressure liquid chromatography; HRMS, high resolution mass spectroscopy; MeOH, methanol; MoA, mechanism of action; MS 4 Å, molecular sieves 4 Å; NMR, nuclear magnetic resonance; **oxoSal**, C20-oxosalinomycin; PMA, phosphomolybdic acid hydrate; ROS, reactive oxygen species; RT, room temperature; **Sal**, salinomycin; TLC, thin layer chromatography; $TMSN_3$, trimethylsilyl azide; UV, ultraviolet

## ■ REFERENCES

(1) Meacham, C.; Morrison, S. Tumour Heterogeneity and Cancer Cell Plasticity. *Nature* **2013**, *501*, 328−337.
(2) Nieto, M. A.; Huang, R. Y.; Jackson, R. A.; Thiery, J. P. EMT: 2016. *Cell* **2016**, *166*, 21−45.
(3) Pattabiraman, D. R.; Weinberg, R. A. Tackling the Cancer Stem Cells − What Challenges Do They Pose? *Nat. Rev. Drug Discovery* **2014**, *13*, 497−512.
(4) Tam, W. L.; Weinberg, R. A. The Epigenetics of Epithelial-Mesenchymal Plasticity in Cancer. *Nat. Med.* **2013**, *19*, 1438−1449.
(5) Thiery, J. P.; Acloque, H.; Huang, R. Y.; Nieto, M. A. Epithelial-Mesenchymal Transitions in Development and Disease. *Cell* **2009**, *139*, 871−890.
(6) Thiery, J. P. Epithelial-Mesenchymal Transitions in Tumour Progression. *Nat. Rev. Cancer* **2002**, *2*, 442−454.
(7) Phi, L. T. H.; Sari, I. N.; Yang, Y. G.; Lee, S. H.; Jun, N.; Kim, K. S.; Lee, Y. K.; Kwon, H. Y. Cancer Stem Cells (CSCs) in Drug Resistance and Their Therapeutic Implications in Cancer Treatment. *Stem Cells Int.* **2018**, *2018*, 5416923.
(8) Prieto-Vila, M.; Takahashi, R. U.; Usuba, W.; Kohama, I.; Ochiya, T. Drug Resistance Driven by Cancer Stem Cells and Their Niche. *Int. J. Mol. Sci.* **2017**, *18*, 2574.
(9) Gupta, P. B.; Onder, T. T.; Jiang, G.; Tao, K.; Kuperwasser, C.; Weinberg, R. A.; Lander, E. S. Identification of Selective Inhibitors of Cancer Stem Cells by High-Throughput Screening. *Cell* **2009**, *138*, 645−659.
(10) Naujokat, C.; Steinhart, R. Salinomycin as a Drug for Targeting Human Cancer Stem Cells. *J. Biomed. Biotechnol.* **2012**, *2012*, 950658.
(11) Kim, K. Y.; Park, K. I.; Kim, S. H.; Yu, S. N.; Park, S. G.; Kim, Y. W.; Seo, Y. K.; Ma, J. Y.; Ahn, S. C. Inhibition of Autophagy Promotes Salinomycin-Induced Apoptosis via Reactive Oxygen Species-Mediated PI3K/AKT/MTOR and ERK/P38 MAPK-Dependent Signaling in Human Prostate Cancer Cells. *Int. J. Mol. Sci.* **2017**, *18*, 1088.
(12) Lu, Y.; Ma, W.; Mao, J.; Yu, X.; Hou, Z.; Fan, S.; Song, B.; Wang, H.; Li, J.; Kang, L.; Liu, P.; Liu, Q.; Li, L. Salinomycin Exerts Anticancer Effects on Human Breast Carcinoma MCF-7 Cancer Stem Cells via Modulation of Hedgehog Signaling. *Chem. Biol. Interact.* **2015**, *228*, 100−107.
(13) Najumudeen, A. K.; Jaiswal, A.; Lectez, B.; Oetken-Lindholm, C.; Guzmán, C.; Siljamäki, E.; Posada, I. M.; Lacey, E.; Aittokallio, T.; Abankwa, D. Cancer Stem Cell Drugs Target K-Ras Signaling in a Stemness Context. *Oncogene* **2016**, *35*, 5248−5262.
(14) Huang, X.; Borgström, B.; Stegmayr, J.; Abassi, Y.; Kruszyk, M.; Leffler, H.; Persson, L.; Albinsson, S.; Massoumi, R.; Scheblykin, I. G.; Hegardt, C.; Oredsson, S.; Strand, D. The Molecular Basis for Inhibition of Stemlike Cancer Cells by Salinomycin. *ACS Cent. Sci.* **2018**, *4*, 760−767.
(15) Lu, D.; Choi, M. Y.; Yu, J.; Castro, J. E.; Kipps, T. J.; Carson, D. A. Salinomycin Inhibits Wnt Signaling and Selectively Induces Apoptosis in Chronic Lymphocytic Leukemia Cells. *Proc. Natl. Acad. Sci. U.S.A.* **2011**, *108*, 13253−13257.
(16) Li, Y.; Shi, Q.; Shao, J.; Yuan, Y.; Yang, Z.; Chen, S.; Zhou, X.; Wen, S.; Jiang, Z. X. Synthesis and Biological Evaluation of 20-*Epi*-Amino-20-Deoxysalinomycin Derivatives. *Eur. J. Med. Chem.* **2018**, *148*, 279−290.
(17) Li, B.; Wu, J.; Zhang, W.; Li, Z.; Chen, G.; Zhou, Q.; Wu, S. Synthesis and Biological Activity of Salinomycin-Hydroxamic Acid Conjugates. *Bioorg. Med. Chem. Lett.* **2017**, *27*, 1624−1626.
(18) Borgström, B.; Huang, X.; Hegardt, C.; Oredsson, S.; Strand, D. Structure-Activity Relationships in Salinomycin: Cytotoxicity and Phenotype Selectivity of Semi-Synthetic Derivatives. *Chem.—Eur. J.* **2017**, *23*, 2077−2083.
(19) Zhang, W.; Wu, J.; Li, B.; Lian, X.; Xia, J.; Zhou, Q.; Wu, S. Design and Synthesis of Conformationally Constrained Salinomycin Derivatives. *Eur. J. Med. Chem.* **2017**, *138*, 353−356.
(20) Huang, M.; Deng, Z.; Tian, J.; Liu, T. Synthesis and Biological Evaluation of Salinomycin Triazole Analogues as Anticancer Agents. *Eur. J. Med. Chem.* **2017**, *127*, 900−908.
(21) Borgström, B.; Huang, X.; Chygorin, E.; Oredsson, S.; Strand, D. Salinomycin Hydroxamic Acids: Synthesis, Structure, and Biological Activity of Polyether Ionophore Hybrids. *ACS Med. Chem. Lett.* **2016**, *7*, 635−640.
(22) Zhang, W.; Wu, J.; Li, B.; Xia, J.; Wu, H.; Wang, L.; Hao, J.; Zhou, Q.; Wu, S. Synthesis and Biological Activity Evaluation of 20-*Epi*-Salinomycin and Its 20-*O*-Acyl Derivatives. *RSC Adv.* **2016**, *6*, 41885−41890.
(23) Shi, Q.; Li, Y.; Bo, S.; Li, X.; Zhao, P.; Liu, Q.; Yang, Z.; Cong, H.; Deng, H.; Chen, M.; Chen, S.; Zhou, X.; Ding, H.; Jiang, Z. X. Discovery of a $^{19}F$ MRI Sensitive Salinomycin Derivative with High Cytotoxicity towards Cancer Cells. *Chem. Commun.* **2016**, *52*, 5136−5139.
(24) Zhang, W.; Wu, J.; Li, B.; Wu, H.; Wang, L.; Hao, J.; Wu, S.; Zhou, Q. Structure-Activity & Structure-Toxicity Relationship Study of Salinomycin Diastereoisomers and Their Benzoylated Derivatives. *Org. Biomol. Chem.* **2016**, *14*, 2840−2845.
(25) Huang, X.; Borgström, B.; Månsson, L.; Persson, L.; Oredsson, S.; Hegardt, C.; Strand, D. Semisynthesis of SY-1 for Investigation of Breast Cancer Stem Cell Selectivity of *C*-Ring-Modified Salinomycin Analogues. *ACS Chem. Biol.* **2014**, *9*, 1587−1594.
(26) Borgström, B.; Huang, X.; Pošta, M.; Hegardt, C.; Oredsson, S.; Strand, D. Synthetic Modification of Salinomycin: Selective *O*-Acylation and Biological Evaluation. *Chem. Commun.* **2013**, *49*, 9944−9946.
(27) Czerwonka, D.; Mielczarek-Puta, M.; Antoszczak, M.; Cioch, A.; Struga, M.; Huczyński, A. Evaluation of the Anticancer Activity of Singly and Doubly Modified Analogues of C20-*Epi*-Salinomycin. *Eur. J. Pharmacol.* **2021**, *908*, 174347.
(28) Czerwonka, D.; Urbaniak, A.; Sobczak, S.; Piña-Oviedo, S.; Chambers, T. C.; Antoszczak, M.; Huczyński, A. Synthesis and Anticancer Activity of Tertiary Amides of Salinomycin and Their C20-Oxo Analogues. *ChemMedChem.* **2020**, *15*, 236.


https://doi.org/10.1021/acsorginorgau.1c00045
ACS Org. Inorg. Au 2022, 2, 222−228

(29) Antoszczak, M.; Urbaniak, A.; Delgado, M.; Maj, E.; Borgström, B.; Wietrzyk, J.; Huczyński, A.; Yuan, Y.; Chambers, T. C.; Strand, D. Biological Activity of Doubly Modified Salinomycin Analogs − Evaluation *in Vitro* and *Ex Vivo*. *Eur. J. Med. Chem.* **2018**, *156*, 510−523.
(30) Urbaniak, A.; Reed, M. R.; Fil, D.; Moorjani, A.; Heflin, S.; Antoszczak, M.; Sulik, M.; Huczyński, A.; Kupsik, M.; Eoff, R. L.; MacNicol, M. C.; Chambers, T. C.; MacNicol, A. M. Single and Double Modified Salinomycin Analogs Target Stem-like Cells in 2D and 3D Breast Cancer Models. *Biomed. Pharmacother.* **2021**, *141*, 111815.
(31) Versini, A.; Colombeau, L.; Hienzsch, A.; Gaillet, C.; Retailleau, P.; Debieu, S.; Müller, S.; Cañeque, T.; Rodriguez, R. Salinomycin Derivatives Kill Breast Cancer Stem Cells by Lysosomal Iron Targeting. *Chem.—Eur. J.* **2020**, *26*, 7416−7424.
(32) Klose, J.; Kattner, S.; Borgström, B.; Volz, C.; Schmidt, T.; Schneider, M.; Oredsson, S.; Strand, D.; Ulrich, A. Semi-Synthetic Salinomycin Analogs Exert Cytotoxic Activity against Human Colorectal Cancer Stem Cells. *Biochem. Biophys. Res. Commun.* **2018**, *495*, 53−59.
(33) Mai, T. T.; Hamaï, A.; Hienzsch, A.; Cañeque, T.; Müller, S.; Wicinski, J.; Cabaud, O.; Leroy, C.; David, A.; Acevedo, V.; Ryo, A.; Ginestier, C.; Birnbaum, D.; Charafe-Jauffret, E.; Codogno, P.; Mehrpour, M.; Rodriguez, R. Salinomycin Kills Cancer Stem Cells by Sequestering Iron in Lysosomes. *Nat. Chem.* **2017**, *9*, 1025−1033.
(34) Huang, X.; Borgström, B.; Kempengren, S.; Persson, L.; Hegardt, C.; Strand, D.; Oredsson, S. Breast Cancer Stem Cell Selectivity of Synthetic Nanomolar-Active Salinomycin Analogs. *BMC Cancer* **2016**, *16*, 145.
(35) Müller, S.; Sindikubwabo, F.; Cañeque, T.; Lafon, A.; Versini, A.; Lombard, B.; Loew, D.; Wu, T. D.; Ginestier, C.; Charafe-Jauffret, E.; Durand, A.; Vallot, C.; Baulande, S.; Servant, N.; Rodriguez, R. CD44 Regulates Epigenetic Plasticity by Mediating Iron Endocytosis. *Nat. Chem.* **2020**, *12*, 929−938.
(36) Deng, Z.; Manz, D. H.; Torti, S. V.; Torti, F. M. Iron-Responsive Element-Binding Protein 2 Plays an Essential Role in Regulating Prostate Cancer Cell Growth. *Oncotarget* **2017**, *8*, 82231−82243.
(37) Schonberg, D. L.; Miller, T. E.; Wu, Q.; Flavahan, W. A.; Das, N. K.; Hale, J. S.; Hubert, C. G.; Mack, S. C.; Jarrar, A. M.; Karl, R. T.; Rosager, A. M.; Nixon, A. M.; Tesar, P. J.; Hamerlik, P.; Kristensen, B. W.; Horbinski, C.; Connor, J. R.; Fox, P. L.; Lathia, J. D.; Rich, J. N. Preferential Iron Trafficking Characterizes Glioblastoma Stem-like Cells. *Cancer Cell* **2015**, *28*, 441−455.
(38) Tornøe, C. W.; Christensen, C.; Meldal, M. Peptidotriazoles on Solid Phase: [1,2,3]-Triazoles by Regiospecific Copper(I)-Catalyzed 1,3-Dipolar Cycloadditions of Terminal Alkynes to Azides. *J. Org. Chem.* **2002**, *67*, 3057−3064.
(39) Rostovtsev, V. V.; Green, L. G.; Fokin, V. V.; Sharpless, K. B. A Stepwise Huisgen Cycloaddition Process: Copper(I)-Catalyzed Regioselective "Ligation" of Azides and Terminal Alkynes. *Angew. Chem., Int. Ed.* **2002**, *41*, 2596−2599.
(40) Jin, T.; Kamijo, S.; Yamamoto, Y. Copper-Catalyzed Synthesis of *N*-Unsubstituted 1,2,3-Triazoles from Nonactivated Terminal Alkynes. *Eur. J. Org. Chem.* **2004**, *2004*, 3789−3791.
(41) Elenbaas, B.; Spirio, L.; Koerner, F.; Fleming, M. D.; Zimonjic, D. B.; Donaher, J. L.; Popescu, N. C.; Hahn, W. C.; Weinberg, R. A. Human Breast Cancer Cells Generated by Oncogenic Transformation of Primary Mammary Epithelial Cells. *Genes Dev.* **2001**, *15*, 50−65.
(42) Morel, A. P.; Lièvre, M.; Thomas, C.; Hinkal, G.; Ansieau, S.; Puisieux, A. Generation of Breast Cancer Stem Cells through Epithelial-Mesenchymal Transition. *PLoS One* **2008**, *3*, e2888.


https://doi.org/10.1021/acsorginorgau.1c00045
*ACS Org. Inorg. Au* 2022, 2, 222−228